GIG Research Institute

JOURNAL OF SUSTAINABLE MINING

Volume 19 | Issue 1 Article 1

2020

Effect of an eccentric decoupled charge on rock mass blasting

Effect of an eccentric decoupled charge on rock mass blasting

Jung-Gyu Kim [a], Mahrous A.M. Ali [b], Jong-Gwan Kim [a,*]

[a] Department of Energy and Resources Engineering, Chonnam National University, Korea
[b] Mining and Petroleum Eng. Depart, Faculty of Engineering- Al-Azhar University, Qena, Egypt

Abstract

Experimental and numerical analyses were conducted to investigate the effect of an eccentric loaded contour hole on a rock mass. In the concrete blocks used for the analyses, detonating cords were placed at the centre of the blast hole and eccentrically against the wall of the blast hole. PFC^{2D} and AUTODYN were used for the numerical analyses, and the results of these software showed that an eccentric decoupled charge can result in the directional development of fractures, thereby enabling the control of cracks in the opposite direction. Even though both types of blasting have identical decoupling indexes, the crack and fracture patterns were affected by the location of the explosive, tamping, and other conditions. The results showed that an eccentric charge holder can be applicable to control the fracture direction and the damaged zone. For an eccentric charge, the initial crack was generated at 0.01 ms and expanded in the intended direction. For the eccentric charge, the maximum pressure at the area in contact with the blast hole wall exceeded that for the central decoupled charge by a factor of 5.5. Furthermore, the pressure in the intended direction was twice of that in the opposite direction.

Keywords: eccentric decoupled charge, fracture pattern, PFC, AUTODYN, decoupling index

1. Introduction

Several experimental studies have been conducted to analyze the dynamic mechanical behavior of materials and structures. A semi-disc dynamic three-point bending test involving impact loading was conducted in a previous study; the results showed that the dynamic loading rate has a significant influence on the fracture toughness and arrest toughness of materials [1, 2]. Smooth blasting, which is the controlled blasting typically used for tunnel excavations, is based on decoupling effects. However, the blasting pressure radiates in all directions, including the wall and the free surface. The use of eccentric charges is an ideal method to reduce the damage caused to the final wall and to concentrate the energy toward the free face, for a well fracture [3–5]. Our experiment is the initial work aimed at controlling the charge based on an analysis of the geological setting, which elucidates the direction of the charge, based on whether the drilling is deep or semi-deep. A majority of these studies have examined the column removal scenario, wherein one of the columns is removed, and the load of this column is applied vertically on the upper face to assess the behavior of the frame until failure [6, 7]. Decoupled charges are generally adopted to minimise the damage zone on the final wall. The decoupling index is the ratio of the blast-hole diameter and the explosive diameter. The space between the wall and the explosive acts as a cushion and prevents the dynamic force from acting directly on the wall. Explosives are loaded at the centre of the hole and are not in contact with the wall [8]. Researcher indicted the relationship between burden and borehole diameter which is linear. Also, he

Received 21 January 2020; revised 12 March 2020; accepted 13 March 2020.
Available online 5 October 2020

* Corresponding author.
E-mail address: kimjg@jnu.ac.kr (J.-G. Kim).

https://doi.org/10.46873/2300-3960.1000

carried out burden in underground mine were lower than in surface mine which related to higher ore densities, greater confinement in blasting and finally greater demand for wall fragmented rock [9]. Cost and saving time are the main target for using Measurement while drilling (MWD) techniques. This technique provides a useful tool to manage drill and blasting in surface mining also, improve the reliability of the blast design by providing the drill and blast engineer with the information specially tailored for use. From this, decisions can be made on the most appropriate type and amount of explosive charge to place in a per blasthole or to optimize the interhole timing detonation time of different decks and blastholes [10,11]. An improved blasting operation depending on blast pattern to modified fragmentation related to drilling logs. Many factors recorded during drilling operations with analyzed. Author mentioned the rock blastablity and determined the rock quality index as index for rock characterization. Two methods for the powder factor determination are suggested and their uses illustrated. Better knowledge of bench geology and structure will allow a better evaluation of zones' blastability and a timely blast design modification, and will therefore facilitate production and processing processes and reduce the operation cost [12]. They discussed on blast fragmented with assume the rock properties. They used stochastic modeling approach to quality the variation. This model used thousand iteration, generates a statistical representation of the expected fragmentation resulting from a production blast. The various blast-related parameters influence different parts of the fragmentation distribution, e.g., rock strength and explosive velocity of detonation have most impact on the fines. The technique is used to identify the parameters that have the greatest influence on various size fractions. Such an analysis will be useful to direct resources to efficiently minimise the variation [13].

In this study, an eccentric charge was used to maximize the decoupling effect to the final wall and to concentrate the blasting energy toward the free face. By loading the charges toward the free face, the side wall blasting energy is concentrated in the direction of the free face. The final wall on the opposite side has a greater stand-off than that under normal decoupling and consequently should be protected properly. The damages to the wall and the free surface were compared for two different types of charges: centrally decoupled charges and eccentrically decoupled charges. Cylindrical concrete models were blasted, and the corresponding numerical models were simulated using PFC(Particle Flow Code)^{2D} and AUTODYN software to investigate pressure concentration and fracture propagation [14,15]. The damaged or disturbed rock zone (DRZ) is defined as the alternating zone induced by mechanical, thermal, hydraulic, or chemical processes. The resulting modulus, hydraulic conductivity, and seismic velocity differ from the original values. The DRZ includes the failure zone, damaged zone, and disturbed zone. If the DRZ is caused due to excavation, it is termed as the excavation disturbed or damaged zone (EDZ). Even though the disturbance and damage are not clearly defined, their features and areas are mainly dependent on the excavation method, size of the structure, rock strength, and initial stress. The EDZ is the rock zone around an underground excavation where irreversible changes occur. Such zones are inevitable because of the changing conditions resulting from the removal of rock during the construction process. As EDZ zone exists deeper in the rock; in this zone the changes associated with construction are reversible. Previous studies have focused on crack/fracture evolution and the distinction between the mechanical and flow EDZ to establish the extent to which a coupled model is required [16–19].

2. Experimental work

This section describes the preparation of the materials, different blast-hole designs, models, and investigation of the experimental results. Five cases A, B, C, D, and E were tested, and the results were evaluated to determine if fracture is generated in the intended direction by eccentric decoupling [20]. Normal Portland cement was used for a concrete cylinder model, according to concrete quality standards (KS L 5201). To enhance the durability and strength of the concrete cylinder model, an air entraining water reducing admixture was added, according to the chemical admixture standards (KS F 2560). Furthermore, detonating cords of 10 g/m and 20 g/m were used. Five concrete cylinders, with a diameter and length of 20 cm and 40 cm, respectively, and a ∅45-mm blast hole, were cured for 28 days and set in the ground. Styrofoam and circular plastic films were used to fix the detonation cords to the centre or on the sidewalls. Fig. 1 depicts the

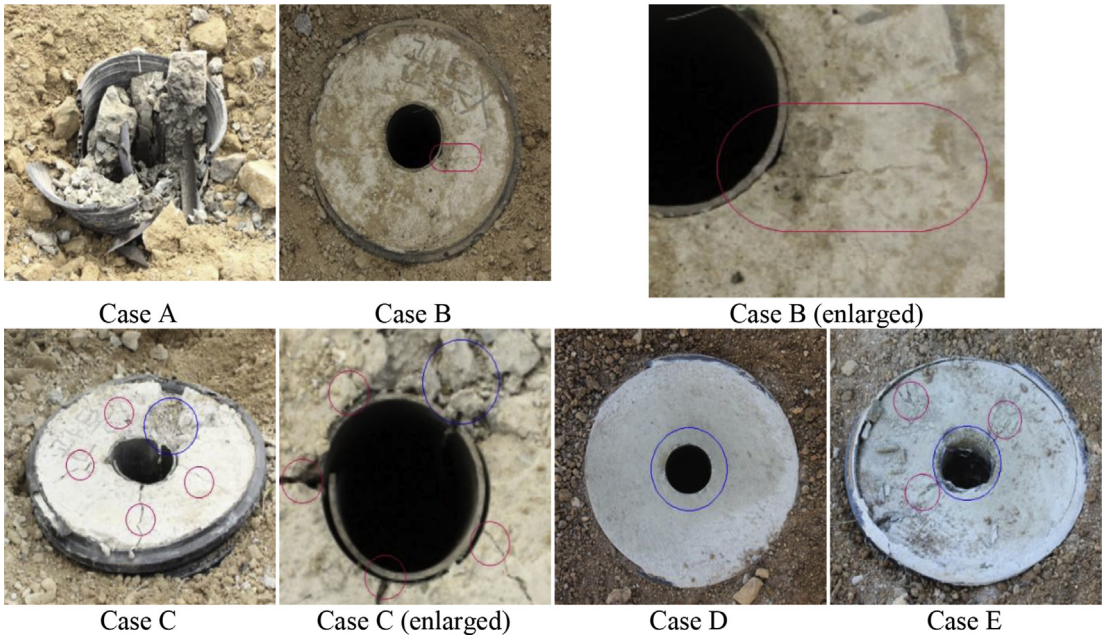

Fig. 1. Fracture pattern after blasting.

fracture patterns obtained when a 20 g/m detonating cord was eccentrically loaded on the sidewall of the hole and blasted (Case A). The hole was stemmed, and it completely fractured, as shown in Fig. 1. In Case B, the concrete cylinder was eccentrically loaded with a 10 g/m detonating cord and blasted. Fine cracks were generated at the point of contact of the detonating cord. Additional cracks were not observed, except at the blast point. Case C involved eccentrically loading the concrete cylinder with a 20 g/m cord and blasting it. Several evident cracks were generated from the hole in the radial direction, and some portion of the collar was crushed around the contact point. In Case D, the concrete cylinder was blasted with a central-loaded 10 g/m cord. No cracks were generated on the cylinder wall, and only small parts around the collar of the hole were evenly crushed. In Case E, the concrete cylinder was blasted with a central-loaded 20 g/m detonating cord. Three crack lines were observed on the surface, and some parts of the collar were fractured [21,22]. Thereafter, the results of these five cases that were blasted under different conditions were compared. Cases A and C had the same amount of explosive; however, stemming was only performed in Case A. Thus, the results indicate additional fracturing in Case A, as compared to Case C. The tests on Cases B and E were conducted using the same amount of explosives, and both cases illustrated that the additional cracks and fractures were generated in the case wherein the detonating cord was located on the sidewall of the hole, as compared to the cracks generated when the detonating cord was located at the centre. Table 1 presents the results of each experiment.

3. Numerical analyses

The damaged zones can be analyzed via numerical analyses, using PFC^{2D}, which employs the DEM (Distinct Element Model), and AUTODYN^{2D}, which employs the FEM (Finite Element Model). Both these software were used to verify the effect of eccentric charges based on a comparison of the damaged zones [23], so numerical analyses were carried out using these software in this study.

Table 1. Experimental results.

Case	Stemming	Detonating Cord (g/m)	Charging method	Result
A	○	20	Eccentric	Crushed to parts
B	×	10	Eccentric	1 crack
C	×	20	Eccentric	5 cracks Crushed (sidewall)
D	×	10	Central	–
E	×	20	Central	3 cracks Crushed (around)

Table 2. Determined micro-parameters for generating a cement mortar block.

Micro-parameter	Unit	Value	Micro-parameter	Unit	Value
specific gravity(ρ)	g/cm^3	2.3	F (mean of σ_c)	MPa	80
r_{min}	mm	1.5	G (mean of τ_c)	MPa	80
μ	–	0.5	H (s.d./mean of σ_c, τ_c)	–	0.2
E_c	GPa	52	SFn	–	0.2
kn/ks	–	2.45	SFs	–	0.2

3.1. PFC^{2D}

PFC^{2D} is the distinct-element modeling software provided by Itasca. It was used to verify the effect of eccentric charges by comparing the damaged zones. The material characteristics of concrete and the detonating cord were determined using the micro-parameters listed in Table 2. The fracture patterns and stress for the centrally loaded and eccentrically loaded cases were compared.

SF is the scale factor. SFn is the value multiplied by the average vertical strength (F), and SFs is the value multiplied by the average shear strength (G). According to the change in the SF, Young's modulus, Poisson's ratio, uniaxial compressive strength, and the crack initiation strength of cement mortar were calculated and applied at SF 0.2. σ_c is the average vertical strength of the contact bond, τ_c is the average shear strength of the contact bond, and H is the ratio of the standard deviations of the average vertical and shear strengths of the contact bond. Eight factors, except the scale factors (SFn and SFs), were the variables that define the constituent particles and contact characteristics of the analytical PFC model.

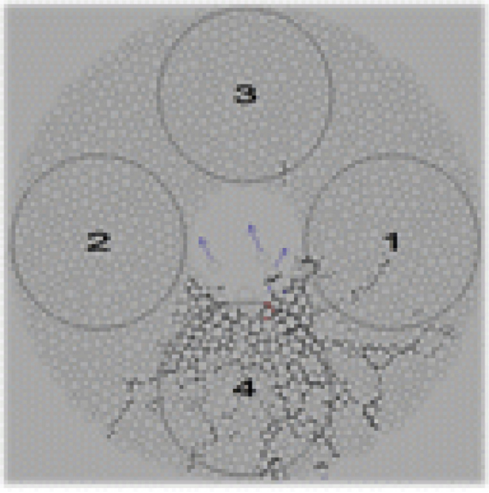

Fig. 2. Investigation areas.

The blasting source was simulated by applying pressure control to the surrounding wall, according to the change in the size of the particles in the blasting hole. The blasting source was fixed, and the vibration history was monitored. The porosity, disconnection of chains, and stress components were investigated for two loading cases, for the circular investigation areas with a diameter of 75 mm around the blast hole (Fig. 2).

3.1.1. Crack propagation

The crack propagation patterns for the five cases are depicted in Fig. 3. The cracks were generated until 5 ms after detonation. The blasting pressures are fully decayed, and no cracks were generated after 5 ms. The lower point of the hole was the eccentric loading point.

3.1.2. Blasting-induced stress

The blasting-induced stress (σ_{xx}, σ_{yy}) were determined, as shown in Fig. 4. The eccentrically loaded cases exhibited a significant difference between the stress components, whereas the centre-loaded holes have approximately identical components. This phenomenon can be attributed to the asymmetrical loading conditions, which can be a favorable condition for shear failure.

"Up" refers to the portion away from the detonating cord when the sidewall is loaded, and "Down" refers to the portion where the detonating cord is attached. The X axis represents time, and the Y axis represents stress and porosity. A two-dimensional stress field is assumed for the PFC model. The two-dimensional analysis did not consider ignition in the vertical direction and ignored the velocity of detonation of the detonating cord. The model is a simple radial load model.

3.1.3. Porosity change

The porosity is changed due to crack development. Even though the cracks were not developed, and the pores were not well expanded, the difference between the two loading methods is evident because of the low pressures observed in Cases B, D and E (Fig. 5). In the figure, 0.156 indicates 15.6% and not 0.156%. The general porosity of concrete is 15–20%; hence, the PFC model is adequate. In general, it is known that the porosity and permeability are linear [24], and the crack propagation is performed in a direction in which the porosity of the concrete material is large. Therefore, it can be estimated that the greater the permeability of the material, the better the crack propagation.

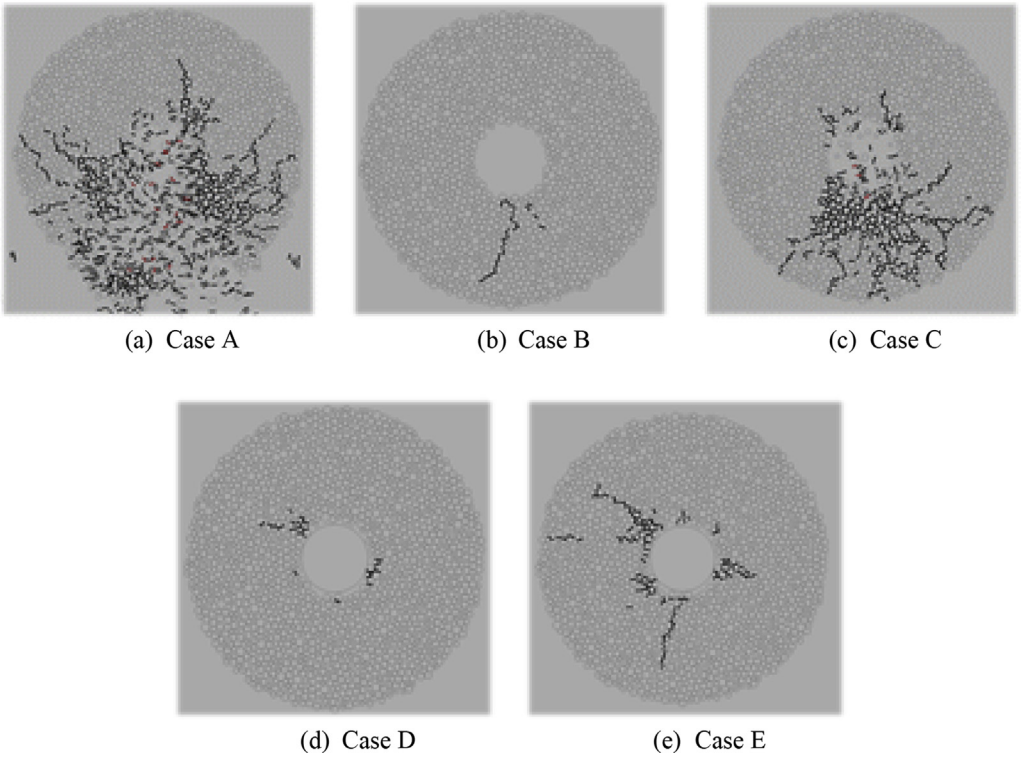

Fig. 3. Generated cracks.

The numerical analysis of the eccentrically decoupled holes indicates greater fracture growth, higher porosity between the particles, and greater pressure propagation in the intended direction, as compared to that in central decoupling.

3.2. AUTODYN^{2D}

The specific features and capabilities of AUTODYN^{2D} are described in this section. In particular, the software incorporates all the function required

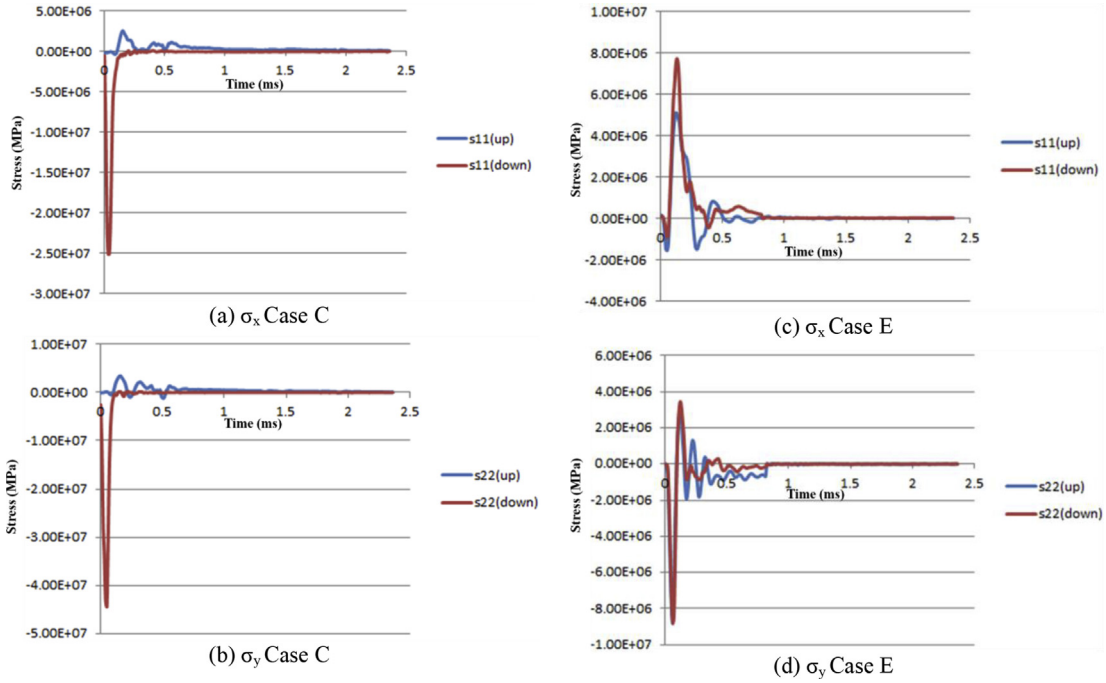

Fig. 4. Typical stress - time history acting on the measuring area.

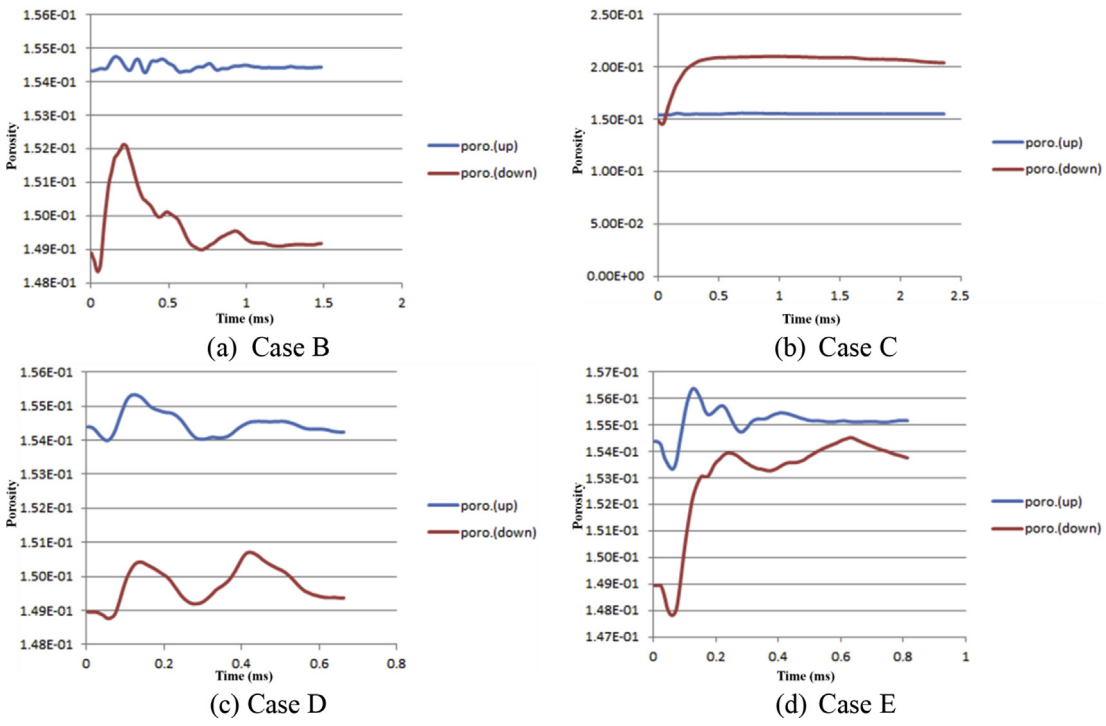

Fig. 5. Porosity – time history acting on the measuring area.

for the generation of a numerical model, analysis, and display of results in a single graphical menu-driven package. The codes can be compiled at the same functionality, albeit at varying speeds, on personal computers and engineering workstations as well as mainframes and supercomputers.

The central and eccentric charges in the cylinder holes were simulated using the hydro code of AUTODYN. PETN was selected as the charge equivalent of the detonating cord. The corresponding material properties for concrete are listed in Table 3. The boundary condition was set as "transmit" for infinite radiation.

3.2.1. Crack propagation

The damage level until 0.05 ms after detonation is depicted in Fig. 6. In the central detonation case, radial and even propagation of cracks was observed, according to the stress wave radiation. Conversely, the eccentric charge yielded crack generation at the contact point, 0.01 ms after detonation. Moreover, crack expansion was prevalent toward the intended direction in the right side. 1. The boundary condition between the concrete cylinder model and the external atmosphere is not clearly stated in the paper. However, in the analysis for evaluating the impact of failure, the concrete cylinder and the external atmosphere are generally set to free surfaces.

When the blast pressure propagates through the blast hole in the cylinder, the compression wave proceeds along the concrete cylinder, which is a solid material, and the free surface reaches the free surface, tensile stress waves are formed due to the difference between the impeller and the solid material. These tensile stress waves induce the tensile failure of the concrete cylinder, thereby extending the crack in the concrete cylinder between the blast source and the artificial joint.

3.2.2. Pressure change

Gauge points were assigned along the intended direction at 10 mm-intervals to observe the changes in the stress during the first 0.1 ms (Fig. 7). The maximum pressure of gauge #2 for the central charge was 31 MPa at 0.012 ms, whereas it was 170 MPa at 0.004 ms in the case of the eccentric charge, at the same position. Additionally, the other

Table 3. Input parameters for applied model.

Equation of state	Strength model		Failure model
	RHT concrete		RHT concrete
P-alpha	Shear modulus	16.7 GPa	Tensile failure
	Compressive strength	35 MPa	
	Tensile strength	3.5 MPa	
	Shear strength	6.3 MPa	

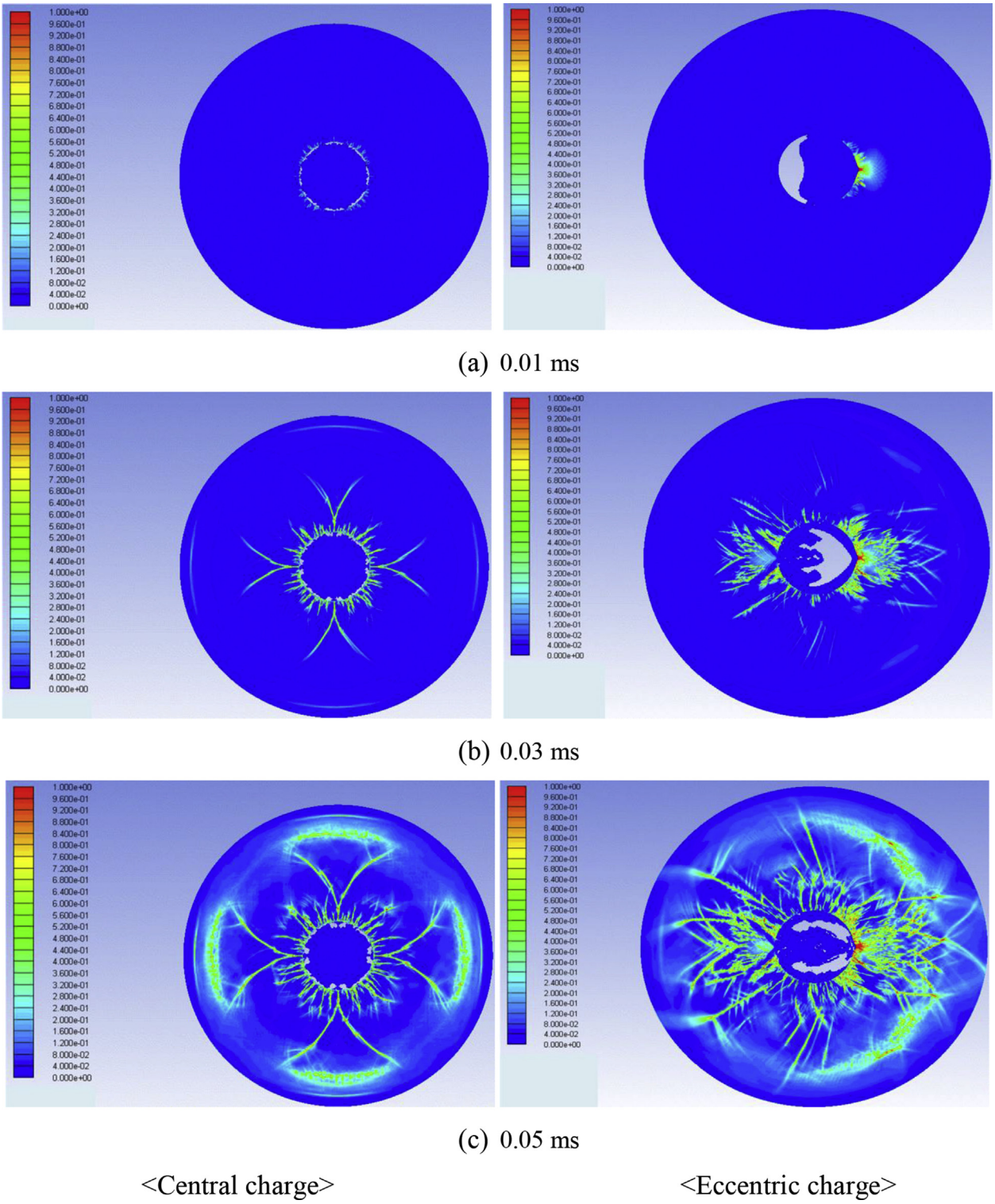

Fig. 6. Crack propagation patterns of central and eccentric charges.

gauges indicate higher pressures for the eccentric charge case, as compared to the central charge case.

The stress time history can be caused by reflected waves; however, it can also change depending on the type of gauge used in the analysis. In AUTODYN, the purple gauges are moving gauges, unlike the gauges, which are fixed to nodes. It indicates the pressure value entering the

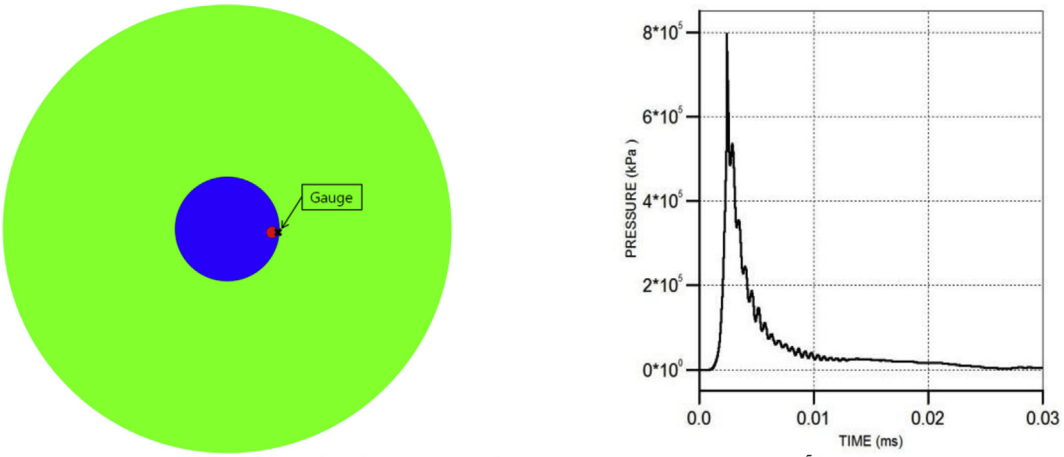

(a) Eccentric charge case (Max. pressure: 7.960×10^5 kPa)

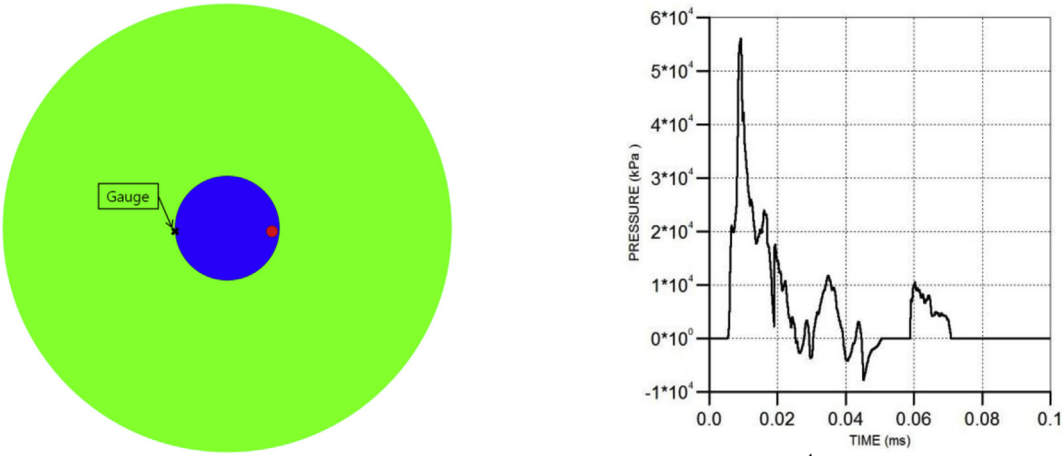

(b) Eccentric charge case (Max. pressure: 5.607×10^4 kPa)

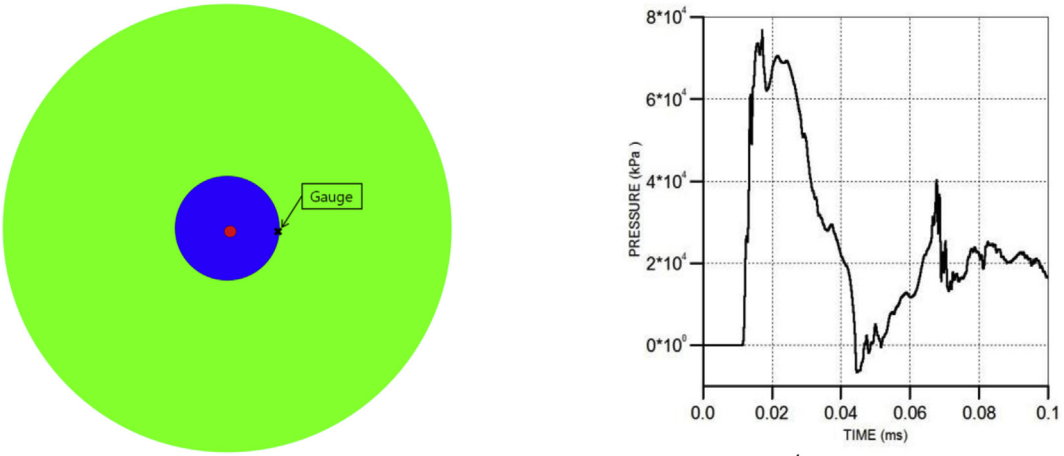

(c) Central charge case (Max. pressure: 7.677×10^4 kPa)

Fig. 7. Time history of the pressure at the cylinder wall.

node (location at which the movement occurs) and not the resultant value of the defined position. The moving gauges may cause fluctuations in the pressure value.

3.2.3. Stress distribution

Fig. 8 presents the crack development, pressure contours, and pressure distribution toward the intended side and the opposite side, 0.05 ms after

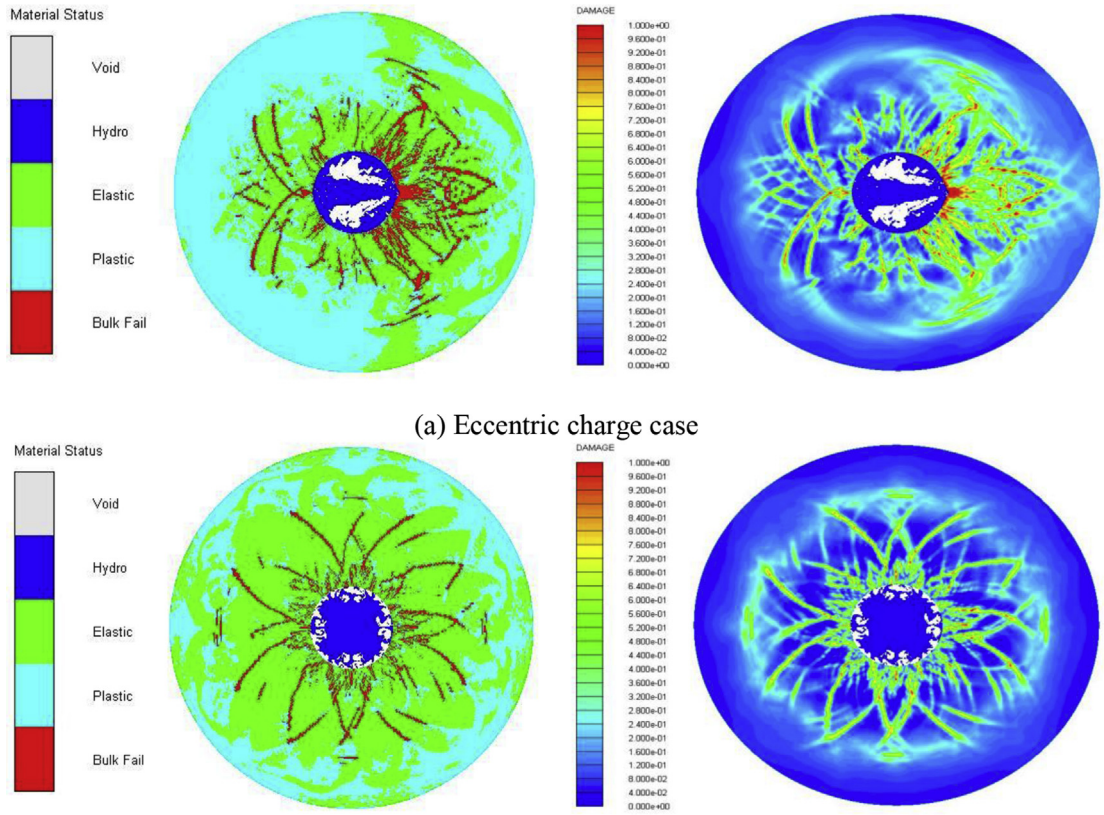

Fig. 8. Cracks and pressure distribution.

detonation, to compare the failure states. Several cracks are induced at the charged (intended) side by the initial stress wave. The pressure distribution at the intended side also exhibits a wider high-pressure zone than that in the opposite direction. The maximum pressure in the intended direction attains a value that is twice of that in the opposite direction.

The AUTODYN^{2D} analysis demonstrates that the stress wave was directly applied on the wall at the contact point of the perimeter, and the initial cracks were generated more easily and developed well in the intended direction for the eccentric case, than that in the central charge case. This indicates that, by using an eccentric charge, the initial crack generation and fracture development can be controlled in the intended direction and consequently fragmented to the free surface, while ensuring that the opposite final wall is protected, similar to the central decoupled holes.

4. Conclusions

Experiments and numerical analyses of eccentric charges for contour holes were conducted with an aim to reduce the damage caused to the rock wall as well as to control the direction of crack generation toward the free surface. In this study, centrally and eccentrically charged concrete cylinder models were blasted. Furthermore, PFC^{2D} and AUTODYN^{2D} analyses were conducted for these models to verify the controlled decoupling effects. The results of this study are summarized as follows:

1) The experimental results show that eccentric charges produce more cracks and fractures than central charges, with more cracks being generated in the intended direction than in the opposite direction.
2) The results of the PFC^{2D} analysis agree with the experimental results. Additional cracks were generated and developed in the intended direction, resulting in fracture expansion and increased porosity. The differential stress in the eccentric case was higher than that in the central charge case, which indicates that shear failure occurs easily.
3) The results of the AUTODYN analysis show that decoupling in the central charge causes a radial generation of cracks. Conversely, in the eccentric charge case, it indicates an initial crack

generation at 0.01 ms and expansion in the intended direction. The maximum pressure in the eccentric case exceeded that in the central charged case by a factor of 5.5. The pressure in the intended direction was twice of that in the opposite direction.

4) The results of the experiments and numerical analyses show that high stress and initial fractures can be generated in the intended direction by using eccentric decoupling. Although the same decoupling index was applied in both cases, the shock wave and initial fracture could be concentrated toward the free face via eccentric loading, while ensuring that the damage caused to the bed rock was minimized.

Conflicts of interest

None declared.

Ethical statement

Authors state that the research was conducted according to ethical standards.

Funding body

None.

References

[1] Sołtys A, Twardosz M, Winzer J. Control and documentation studies of the impact of blasting on buildings in the surroundings of open pit mines. J Sustain Mining 2017;16(2017):179e188.
[2] Zhang QB, Zhao J. Effect of loading rate on fracture toughness and failure micromechanisms in marble. Engin Fract Mechan 2013;102:288–309.
[3] Fairhurst C. "Proc. Int. Workshop on rock mechanics of nuclear waste repositories" 1-44. American Rock Mech. Assoc; 1999.
[4] Yang HS, Kim JG, Ko YH, Noh Y, Shin MJ. Explosives & blasting". J. KSEE) 2014;32:1–4.
[5] Yang Y, Shao Z, Mi J, Xiong X. Effect of adjacent hole on the blast-induced stress concentration in rock blasting. Hindawi Adv Civil Engin 2018;2018:13. https://doi.org/10.1155/2018/5172878. Article ID 5172878.
[6] Mousa HG. Collapse analysis of a reinforced concrete frame due to middle column loss by explosion. Civil Environ Engin 2018;8:3. https://doi.org/10.4172/2165-784X.1000311. 2018.
[7] Yang R, Xu P, Yue Z, Chen C. Dynamic fracture analysis of crack-defect interaction for mode I running crack using digital dynamic caustics method. Engin Fracture Mech 2016;161:63–75.
[8] Basravi A. Finite element analysis of reinforced concrete column with longitudinal hole. Faculty of Civil Engineering University Tektologi Malaysia; 2010.
[9] Agne RR. Int J Surf Min Reclamat Environ 2007;6(1992):1993.
[10] Segui JB, Higgins M. Blast design using measurement while drilling parameters" fragblast. Int J Blast Fragmen 2010;6(3–4):287–99. 2002.
[11] Smith B. Improvements in blast fragmentation using measurement while drilling parameters", fragblast. Int J Blast Fragmen 2010;6. 2002 - Issue 3-4.
[12] Yin K, Liu H. Using information extracted from drill data to improve blasting design and fragmentation. Fragblast Int J Blast Fragmen 2010;5(3):157–79. 2001.
[13] Thornton D, Kanchibotla SS, Brunton I. modelling the impact of rockmass and blast design variation on blast fragmentation. Fragblast Int J Blast Fragment 2010;6(2):169–88. 2002.
[14] Itasca Consulting Group, Inc.. PFC2D manual: Optional features. Minnesota, USA: Itasca Consulting Group Inc.; 2004.
[15] ANSYS Inc. "ANSYS AUTODYN user's manual", ver. 13 ANSYS inc. 2010.
[16] Dusseault MB, Nawrocki PA. Modelling of damaged zones around openings using radius-dependent Young's modulus. Rock Mech Rock Engin 1995;28(4):227–39.
[17] Saiang D. "Behaviour of blast-induced damaged zone around underground excavations in hard rock mass" doctor of philosophy in rock mechanics and rock engineering. 2008.
[18] Fracture Systems Ltd. "Excavation damaged zones assessment" NWMO DGR-TR-2011-21. 2011.
[19] Zhu T, Huang D. Influences of the diameter and position of the inner hole on the strength and failure of disc specimens of sandstone determined using the Brazilian split test. J Theoret Appl Mechan 2019;57(1):127–40 (warsaw).
[20] Choi BH. New explosion modeling and its application to concrete column blasting using PFC. PhD thesis. Chonnam National Univ; 2005.
[21] Chang S-H, Chung-In L, Lee Y-K. "An experimental damage model and its application to the evaluation of the excavation damage zone" rock. Mech. Rock Engng. 2007;40(3):245–85.
[22] Zhao L, An X, Liu F, Zhang J, Hu N. "Secondary bending effects in progressively damaged single-lap single-bolt composite joints" Results in Physics. 2016.
[23] Zhou J-W, Yang X-G, Xing H-G, Xue Y-F, He G. Assessment of the excavation-damaged zone in a tall rock slope using acoustic testing method. Geotech Geol Eng 2014;32:1149–58.
[24] AlHomadhi ES. New correlations of permeability and porosity versus confining pressure, cementation, and grain size and new quantitatively correlation relates permeability to porosity. Arab J Geosci 2014;7:2871–9.